Resistivity and Hall effect in sputtered Nb/Ni multilayers

M. T. Pérez-Frías and J. L. Vicent
Departamento Física de Materiales, Facultad de Ciencias Físicas, Universidad Complutense, 28040 Madrid, Spain
(Received 14 March 1988; revised manuscript received 20 June 1988)

Multilayered samples of Nb/Ni have been fabricated by dc triode sputtering. X-ray diffraction patterns were obtained in the reflection geometry. Small-angle data show several order peaks and subsidiary maxima, indicating strong composition modulation. ω-rocking curves at small angle are sharp, with $\Delta\omega \sim 0.1°$. High-angle scans do not show superlattice peaks. The samples have (110) texture for Nb and (111) texture for Ni. Multilayered systems with severe structural size mismatch are incoherent, and Nb/Ni multilayers are among these incoherent systems. Resistivity measurements show logarithmic minima at low temperature. These minima depend on bilayer thickness, shifting, and deepening to a higher temperature with decreasing modulation wavelength. Their origin could be due to weak localization. We have explored the contribution of Ni and Nb layers to this resistivity effect. The role of Ni layers is unclear at present, but we can rule out a modified Kondo mechanism. However, the short mean free path of the conduction electrons in Nb layers, estimated from Gurvitch's model, could play a clear role in this weakly localized regime. The Hall effect in Nb/Ni multilayers shows a clear ferromagnetic character with very well-defined ordinary, R_0, and extraordinary, R_s, coefficients. The samples have saturation magnetizations and hysteresis loops down to nominal 10-Å layer thickness of Ni. The Hall-effect data could be a hint of dimensional effects in ferromagnetism. R_0 and R_s are temperature independent between 4.2 and 100 K. R_0 is also bilayer-thickness independent, and the carrier concentration seems to remain constant for a fixed Nb/Ni layer thickness ratio. R_s values show an enhancement in comparison to the R_s value of pure Ni, and they follow the expression $R_s = a\rho + A\rho^2$, typical of itinerant ferromagnetism.

I. INTRODUCTION

In the past few years synthetic superlattices and multilayer structures have been the ideal test for many interesting physical phenomena.[1] Among different artificially layered materials, metallic superlattices[2] have been used as perfect tools to study, for example, dimensionality problems[3] related with either the variable length scales of the physical properties or collective effects due to the repetitive nature of multilayers.[4]

Many different experimental measurements have been done in metallic multilayers. Electrical transport phenomena have received most of the attention of the workers in the field. Resistivity data are published in most reports of metallic multilayers available in the literature, with Hall-effect measurements reported very few times.[5]

Recently the theoretical study of Bauer and van der Merwe[6] shows that Nb/Ni could be a good candidate among different possibilities to grow crystalline superlattices. In this paper, we present results on the fabrication, structure (using x-ray diffraction), resistivity, and Hall effect in Nb/Ni multilayers.

The samples were grown by dc triode sputtering. X-ray experiments were done in the normal reflection geometry and these results show good layering of the samples. Electrical transport effects were measured between 4.2 and 300 K for resistivity and 10 and 100 K with applied magnetic field up to 7 T for the Hall effect. Resistivity data show the role of the short electronic mean free path and possible localization effects, while the Hall-effect data show the ferromagnetic character of the samples down to very short nominal thicknesses of the Ni layers.

II. EXPERIMENTAL METHODS

Nb/Ni multilayers were grown by dc triode sputtering in the usual way[2] with appropriate shutters, by alternately depositing Nb and Ni layers using two independent cathodes and stopping the substrates in front of the Nb and Ni cathodes alternately. The base pressure was 5×10^{-7} torr. The sputtering gas was pure Ar (99.998%) and its pressure during deposition was 0.5 mTorr. The films were deposited onto unheated Corning-glass substrates which were previously cleaned with trichloroethylene, acetone, and alcohol for 15 min, each one in an ultrasonic cleaner. The distance between the substrate and the sputtering target was 10 cm. The deposition rate was measured with a quartz-crystal oscillator, being about 0.6 Å s^{-1} for both Nb and Ni. The total thickness of the film was around 2000 Å and it was checked with a Dektak profiler.

Standard x-ray diffraction with the scattering vector perpendicular to the plane of the film was made with a Siemens D-500 diffractometer using Cu Kα radiation. The x-ray experiments were made at room temperature and $\theta/2\theta$ and ω (rocking) scans were obtained.

Standard photolithographic technique was used to etch out a suitable pattern for resistivity and Hall-effect measurements. The etchant was $HF:H_2SO_4:HNO_3:H_2O$

(1:2:2:6). Electrical contacts were made by soldering with pure indium. Transport effects were measured by a standard dc four-probe method using a constant current power supply. Hall-effect measurements were checked by the four-sweep method. A commercial temperature controller with calibrated Pt and carbon glass sensors, and a 7-T superconducting solenoid were used in the experiments.

III. RESULTS AND DISCUSSION

A. Fabrication and x-rays

Multilayers of Nb/Ni have been grown with nominal equal and unequal layer thicknesses. The layer thickness has been changed between 20 and 500 Å for the Nb layers and between 10 and 500 Å for the Ni layers. Thus, for instance, we have prepared a 50-Å-Nb/50-Å-Ni multilayer with nominal thickness for the bilayer $\lambda=100$ Å up to 2000 Å total thickness and 300-Å Nb/10-Å Ni with nominal $\lambda=310$ Å up to 2070 Å total thickness of the film.

The composition modulation wavelength is known from monitoring the deposition rate and the time which the substrate spent in front of each cathode. That nominal λ is tested by measuring the total thickness of the film and counting the number of bilayers deposited. Besides, the λ value could be extracted, for short wavelength, from the x-ray diffraction data.[7] The bilayer λ values obtained by both methods were consistent to within 10%, similar to Ti/Ni and Zr/Ni (Ref. 8) but higher than in Mo/Ni.[9]

X-ray diffraction is crucial to study the structure of multilayers and superlattices. The diffraction pattern of a multilayer shows peaks at small angle coming from the periodic composition modulation. For the thinner bilayer Nb/Ni multilayers, x-ray scans show several orders of diffraction peaks which reveal strong composition modulation. Sometimes it is possible to resolve $M-2$ subsidiary maxima, M being the number of bilayers of the film,[10] between adjacent principal diffraction maxima at small angle. These subsidiary peaks arise as a result of interference between waves diffracted from different bilayers of the sample and they are only visible when M is a small integer. The angular spacing of these pendellösung fringes $\Delta\alpha$ could be used to obtain the total thickness D of the multilayer[11]

$$D=\frac{\lambda_x \sin\theta_B}{\Delta\alpha \sin(2\theta_B)} , \tag{1}$$

λ_x being the x-ray wavelength and θ_B the Bragg angle of one of the principal maxima.

Figure 1 shows the small angle diffraction pattern of a sample with $\lambda=168$ Å. The layered structure of the film is clearly shown with at least five orders of low-angle reflections and their corresponding subsidiary maxima. We have to take into account that the first-order peak is absent because its angular position corresponds to a very low 2θ value and cannot be separated from the direct beam with our x-ray diffractometer.

Substituting in Eq. (1) the experimental values from the diffraction pattern in Fig. 1, with $\Delta\alpha=0.02°$, we obtain

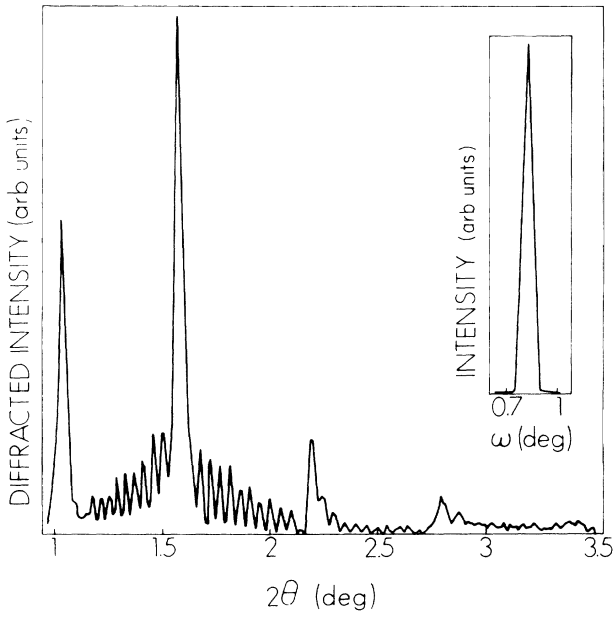

FIG. 1. Small-angle x-ray diffraction pattern for a Nb/Ni multilayer with $\lambda=168$ Å. Rocking curve of the third-order peak in the inset.

the total thickness of the sample $D=2188$ Å which corresponds to a multilayer with $M=13$ and $\lambda=168$ Å. A modulation wavelength of $\lambda=168$ Å and a number of periods equal to 13 are a suitable choice to have a complete picture of the small-angle x-ray diffraction, including the subsidiary maxima. In the inset of Fig. 1 the ω-rocking curve of the third-order peak is shown. For all the samples measured, the typical full width at half maximum (FWHM) is similar for rocking curves of different order peaks, being FWHM about 0.1° (very small undulations of the layers). Another remarkable fact is that the shape of such rocking curves does not show in Nb/Ni superimposed sharp and broad peaks as NbN/AlN and V/Ni (Ref. 12) multilayers do. The very sharp shape of low-angle rocking curves means that Nb/Ni multilayers do not grow with a tilted columnar structure. Finally, the even harmonics at small angle have lower intensities than the odd ones, as can be seen in Fig. 1. That is the expected behavior for an equal layer-thickness sample although there is a deviation from a perfect square-wave composition modulation. The coherence length perpendicular to the layers determined from the FWHM is 1985 Å.

Turning now to high-angle data, first of all we would like to summarize what we expect to occur in the Nb/Ni system. According to Bauer and van der Merwe,[6] this system will be grown fcc on bcc in the Nashiyama-Wassermann orientation. The optimum value for the Nashiyama-Wassermann orientation is $d_B/d_A=0.943$, where d_A and d_B are the nearest-neighbor distances in the (110) and (111) planes for materials A and B, respectively. The Nb/Ni system has $d_{\mathrm{Ni}}/d_{\mathrm{Nb}}=0.871$ and the structural lattice mismatch is 14.8%, very close to the

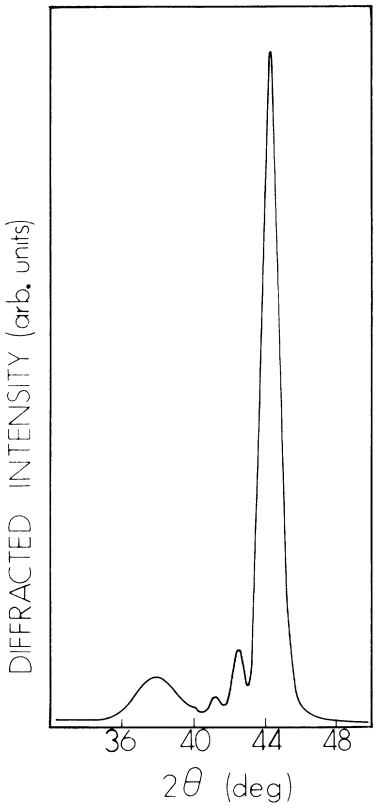

FIG. 2. High-angle x-ray diffraction pattern for a Nb/Ni multilayer with $\lambda = 168$ Å.

limit of 15% for which multilayers do not show high-angle superlattice peaks.[13] Figure 2 shows the high-angle diffraction pattern for the same sample as Fig. 1. The structure of this x-ray $\theta/2\theta$ scan is very similar to the Ti/Ni data in Ref. 13, and the peaks obtained in this high-angle region are associated with scattering from individual Nb and Ni layers with (110) and (111) textures, respectively. Rocking curves show mosaic spread of 3° around the position of the (111) Ni maximum and 8° around the (110) Nb maximum. This larger mosaic spread for the Nb layers could be related to the evolution of the texture with composition modulation wavelength. For the shortest bilayer thickness (40 Å) Nb layers do not show any texture. However, the (111) texture for Ni is still present in unequal layered samples down to 10 Å Ni layer thickness (i.e., 300-Å Nb/10-Å Ni).

A more complete study of the structure of Nb/Ni multilayers will be reported in a forthcoming paper.

B. Resistivity

Resistivity of Nb/Ni multilayers has been measured versus temperature in the range 4.2–300 K for samples with bilayer thicknesses between 40 and 1000 Å. All the samples are metallic and transitions to superconducting states have not been observed down to 4.2 K.

The residual resistivity ratios (RRR) [ρ(300 K)/ρ(4.2 K)] are in the same range (1.2–2) as that for the similar systems Mo/Ni (Ref. 9) and Nb/Cu,[14] and also in the same range as that for the very different system Pd/Co.[15] The highest absolute value of the resistivity at 300 K is 120 $\mu\Omega$ cm for the sample with the thinnest layer thickness, i.e., 20-Å Nb/20-Å Ni, the same that is observed for the 19.2-Å-Mo/19.2-Å-Ni superlattice reported by Khan *et al.*[9] Higher RRR's up to 42 have been found in coherent Nb/Ta multilayers.[16] The lower RRR could be due to impurities in the samples. Auger spectroscopy was made and the samples have mainly N_2, O_2, and C as impurities, but less that 1%. Another possibility could be the very low value of the (pressure x distance) parameter in our sputtering geometry, that is, 4 cm mTorr. That means that there is essentially no thermalization of the atoms.[17]

The Nb/Ni multilayers have the well-known linear dependence[18] ρ(300 K) with $(1/\lambda)$, but we do not reach saturation in the resistivity versus $1/\lambda$ down to the lowest λ which was made (40 Å). The main results of the resistivity measurements are shown in Fig. 3. The thinner-layer samples have a minimum in the resistivity versus temperature whose position deepens and shifts to higher temperature with decreasing λ. A similar behavior was found in the resistivity of Mo/Ni superlattices.[19] Figure 4 shows the logarithmic behavior with temperature of the resistivity below the minimum and the T^2 dependence above the minimum. The origin of this logarithmic temperature dependence could be due to weak localization effects, but when magnetic moments are

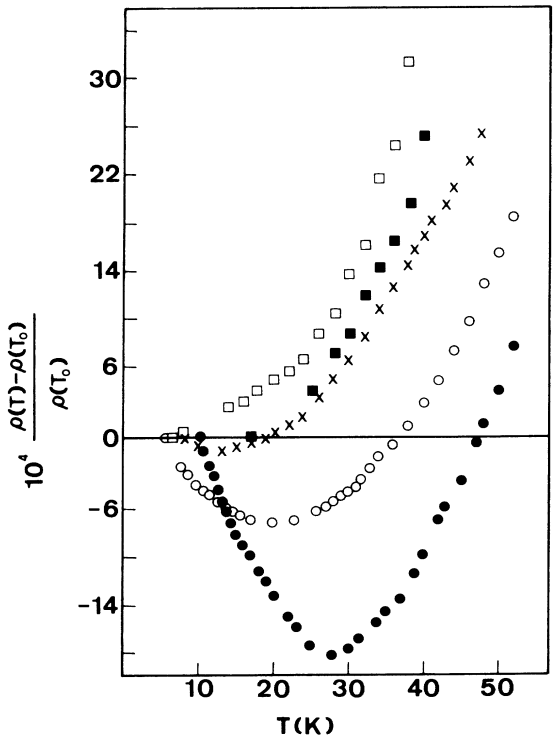

FIG. 3. Normalized resistivity vs temperature for equilayered Nb/Ni films with bilayer thicknesses: ●, $\lambda = 40$ Å; ○, $\lambda = 60$ Å; ×, $\lambda = 100$ Å; ■, $\lambda = 200$ Å; □, $\lambda = 500$ Å; $\rho(T_0)$ being the value of the resistivity at the lowest temperature T_0.

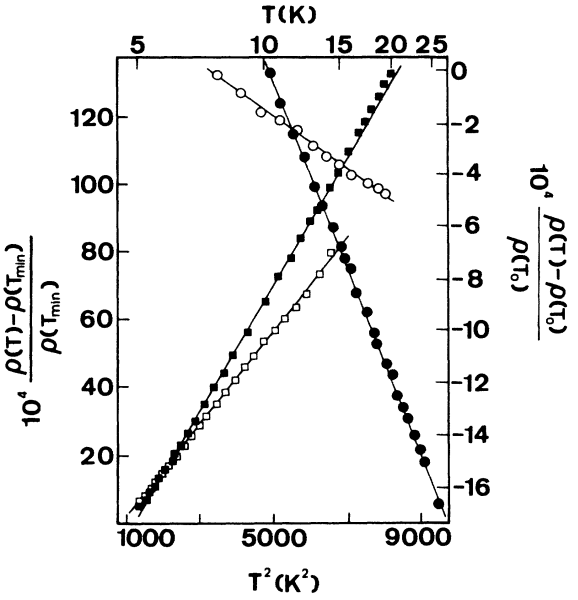

FIG. 4. Logarithmic behavior of the normalized resistivity vs temperature below the minima (top and right side of the figure) for Nb/Ni multilayers with: ●, $\lambda=40$ Å; ○, $\lambda=60$ Å. Normalized resistivity vs square temperature above the minima (bottom and left side of the figure) for the same Nb/Ni multilayers: ■, $\lambda=40$ Å; □, $\lambda=60$ Å; $\rho(T_0)$ being the resistivity at the lowest temperature T_0 and $\rho(T_{\min})$ being the lowest value of the resistivity.

present in a sample, as occurs for Nb/Ni, the Kondo-type mechanism would be a clear candidate to explain the appearance of minima. In our samples, we could have a dilute nickel-based alloy in the interfaces and that could dominate the whole behavior for the shorter bilayer-thickness samples. But then, such a Kondo minimum should disappear when a magnetic field is applied. If we apply a magnetic field up to 7 T, the minima do not change and the only effect that we observe is the magnetoresistance contribution. That means that we can rule out the Kondo effect in our case. All Nb/Ni multilayers are ferromagnetic down to 10-Å nominal thickness of Ni layer, as can be seen in the next section, and so far as we know the interplay of itinerant ferromagnetism and localization is not yet clearly understood. Another possibility could be the modified Kondo mechanism[20] which seems to play a role in the explanation of the resistivity minimum in amorphous ferromagnets. This mechanism includes superexchange interactions mediated by metalloid atoms. In Nb/Ni multilayers the existence of such a superexchange interaction is not clear. In closing, the role of the Ni ferromagnetic layer in the resistivity minima is not well understood.

The Nb layers could also make a contribution to the localization effects, related to the possible short electronic mean free path (MFP) in multilayers. Gurvitch[21] has done a complete study of the resistivity and MFP in metallic multilayered structures. From our experimental data in Nb/Ni multilayers as in most metallic multilayers, the MFP is limited by layer thickness. That means that superlattice effects cannot be observed in electrical transport properties. Following Gurvitch's analysis of resistivity in multilayers, we can treat individual layers as independent resistors connected in parallel. Even this simplified version allows one to see the overall behavior of the MFP in individual layers of a multilayer. All that it is necessary to know in order to perform the study are resistivities at two different temperatures, i.e., at room temperature and at $T=0$, and layer thicknesses. Using Gurvitch's model, we can find the residual resistivity $\rho(0)$ in each individual layer. From the well-known expression

$$\rho(0)L(0)=C' ,$$

C' being a characteristic of each material, we can estimate the low-temperature MFP, $L(0)$. We have used this model to roughly calculate $L(0)$ for the Nb layers in our Nb/Ni system. The value of C' for Nb is based on the lifetime-broadened band structure.[22]

In Fig. 5 the MFP's obtained for Nb in Nb/Ni are shown and compared to the MFP's for Nb in Nb/Al and Nb/Cu from Ref. 21. In Nb/Ni samples, MFP's for Nb are shorter than in the other multilayers. Then it is probable that this very short MFP could play an important role in localization for Nb/Ni multilayers. In Nb/Al, the MFP is longer and localization has not been reported. On the other hand, Nb/Cu presents localization effects[23] but for lower bilayer thicknesses than in Nb/Ni. As was remarked before, Mo/Ni samples[19] exhibit a very similar behavior. We can conclude that the mechanism is not understood. Besides, the ferromagnetic character of the samples obscures the possibility of using magnetoresistance and Hall effect data to distinguish between Anderson's theory[24] and Coulomb correlation[25] as the origin of this weakly localized regime.

C. Hall effect

Figure 6 shows the Hall voltage versus applied magnetic field up to 7 T at low temperature of (a) a nonmagnetic Nb film, (b) a ferromagnetic Ni film, and (c) a multilayer

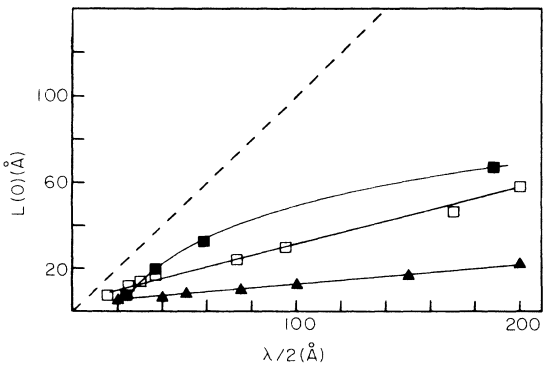

FIG. 5. Low-temperature MFP of Nb vs layer thickness for ■, Nb in Nb/Al; □, Nb in Nb/Cu; ▲, Nb in Nb/Ni multilayers. Nb/Cu and Nb/Al data from Ref. 21.

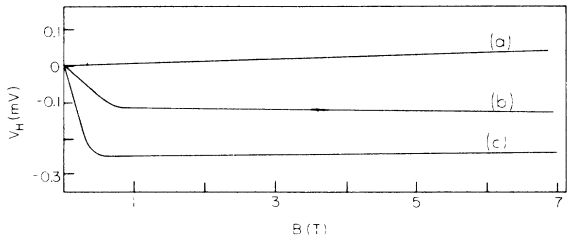

FIG. 6. Hall voltage vs magnetic field for thin films of (a) pure Nb; (b) pure Ni; (c) 300-Å-Nb/10-Å-Ni multilayer at $T=15$ K.

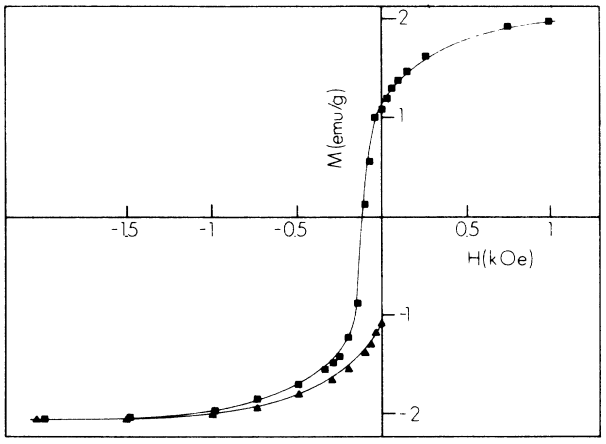

FIG. 7. Hysteresis loop for a 300-Å-Nb/10-Å-Ni multilayer at $T=40$ K: ▲, increasing magnetic field; ■, decreasing magnetic field.

made of ferromagnetic (Ni) and nonmagnetic (Nb) bilayers. This Nb film shows a positive $R_0=1.3\times10^{-10}$ m^3C^{-1} similar to the bulk value reported in the literature.[26] The Ni film shows the typical behavior of a ferromagnetic material:

$$\rho_H=R_0B_z+R_s\mu_0M_z\ ,$$

ρ_H being the Hall resistivity and R_0 and R_s the ordinary and extraordinary Hall coefficients. The values found for the Ni film are $R_s=-0.8\times10^{-8}$ m^3C^{-1} and $R_0=-0.8\times10^{-10}$ m^3C^{-1}, both negative and in the range of the reported values. The 300-Å-Nb/10-Å-Ni multilayer (bilayer thickness 310 Å) also shows a clear ferromagnetic behavior with $R_s=-1.3\times10^{-8}$ m^3C^{-1} and $R_0=+0.4\times10^{-10}$ m^3C^{-1}. We can point out that the Ni contribution is evident in the extraordinary Hall coefficient R_s and the Nb contribution in the sign and value of the ordinary Hall coefficient R_0 in this unequal-layered sample.

The anomalous Hall effect has been used by Bergmann[27] as an extremely sensitive method to detect band ferromagnetism in very thin Ni films. The study of the Hall effect in multilayers (magnetic-nonmagnetic) would be a good method to investigate the proximity effect, long-range magnetic order, and transport parameters.

The ferromagnetic origin of the extraordinary Hall effect has been checked by magnetization measurements using a SQUID magnetometer. These measurements show hysteresis loops and saturation magnetizations down to 10-Å nominal thickness for the Ni layers (see Fig. 7).

One of the indirect methods to measure the magnetization is the Hall effect. The intersection of the two extrapolated straight lines, in the Hall-voltage data (see Fig. 6), defines a point whose abscissa should be equal to the saturation magnetization M_s. Taking into account the Hall effect of Ni in Fig. 6, we get $\mu_0M_s=0.6$ T, but we have to be very cautious when we are dealing with multilayered structures. In these materials we have to take into account their very strong anisotropic structure. Actually the change in slope of the Hall effect means that the saturation applied magnetic field H_s has been reached. For a uniform and isotropic magnetic film, for instance, our pure Ni film, the only anisotropy present is the shape anisotropy and $H_s=NM_s$, N being the demagnetization factor, that is, $N=1$ in the usual geometry for Hall effect in films. But for anisotropic magnetic films, as Nb/Ni multilayers, $H_s=H_K+NM_s$, H_K being the anisotropy field. Therefore, in Nb/Ni samples the Hall effect only provides the H_s values. Figure 8 shows that the temperature dependence of this saturation field H_s strongly depends on the Ni layer thickness. Figure 8 shows that for nominal 10-Å-Ni layer thickness, H_s versus temperature is linear. Due to the fact that $H_s(T)$

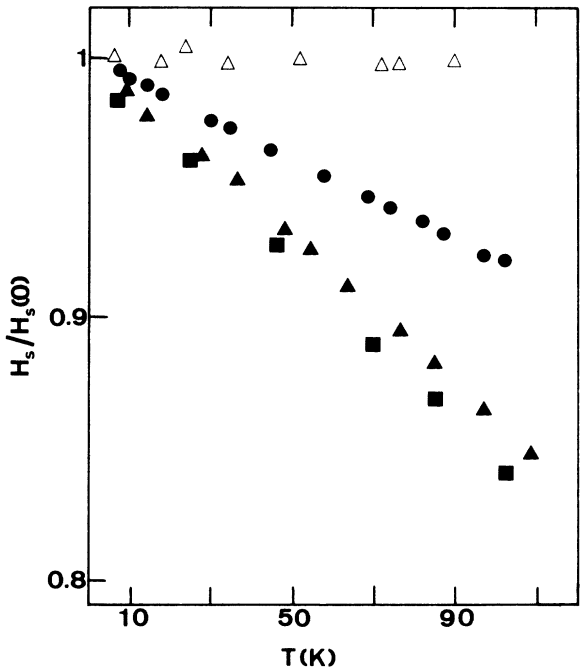

FIG. 8. Normalized saturation field vs temperature for equilayered Nb/Ni film with △, $\lambda=200$ Å and unequal-layer-thickness films; ▲, 300-Å Nb/10-Å Ni; ■, 100-Å Nb/10-Å Ni; and ●, 300-Å Nb/20-Å Ni. $H_s(0)$ being the saturation field at 0 K, obtained by extrapolating to zero the experimental data.

is a function of $M_s(T)$ and $H_K(T)$, a clear explanation of the anomalous temperature dependence of $H_s(T)$ for very short layer thicknesses is not straightforward from the present Hall-effect data.

Several samples were sent out and their saturation magnetizations were measured with a SQUID magnetometer. These measurements show that the samples have an in-plane anisotropy. The temperature dependence of M_s was measured for a sample with $\lambda=200$ Å and for two unequal-layer-thickness samples (300-Å Nb/10-Å Ni and 300-Å Nb/20-Å Ni). Figures 9(a) and (b) show that, while the $M_s(T)$ behavior seems to be similar for all the samples, the $H_K(T)$ data show a clear difference between the highest Ni layer thickness- (100 Å) film and the unequal-layer-thickness films. The 10- and 20-Å nominal-layer-thickness samples have a clear linear $H_K(T)$ behavior, while the film with $\lambda=200$ Å seems to be temperature independent. So far as we know, anisotropy field versus temperature data have not been reported in multilayers. The saturation magnetizations versus bilayer thicknesses behavior is very similar to the Ni/Mo system.[28] The H_K versus layer-thickness data are shown in Fig. 10. We can observe lower values in Nb/Ni than in the Ni/Cu system,[29] but the general trend of the data

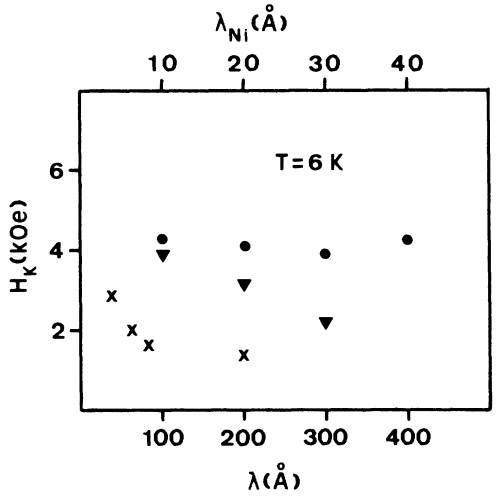

FIG. 10. Anisotropy field vs layer thickness of the films at 6 K; ×, equilayered films (λ being bilayer thicknesses, bottom axis of the figure); ●, unequal layer thicknesses (λ-Å Nb/10-Å Ni, bottom axis of the figure); and ▼, unequal layer thicknesses (300-Å Nb/λ_{Ni}-Å Ni, top axis of the figure).

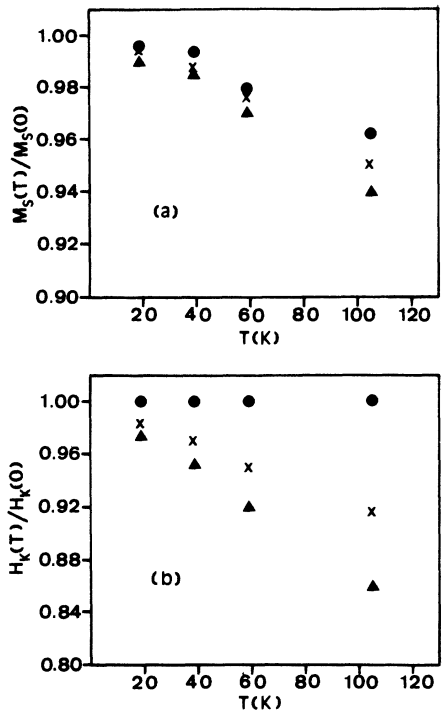

FIG. 9. (a) Normalized saturation magnetization vs temperature for equilayered films: ●, $\lambda=200$ Å and unequal layer-thickness films; ▲, 300-Å Nb/10-Å Ni; and ×, 300-Å Nb/20-Å Ni. $M_s(0)$ being the saturation magnetization at 0 K obtained by extrapolating to zero the experimental data. (b) Normalized anisotropy field vs temperature for equilayered films: ●, $\lambda=200$ Å and unequal layer-thickness films; ▲, 300-Å Nb/10-Å Ni; and ×, 300-Å Nb/20-Å Ni. $H_K(0)$ being the anisotropy field at 0 K obtained by extrapolating to zero the experimental data.

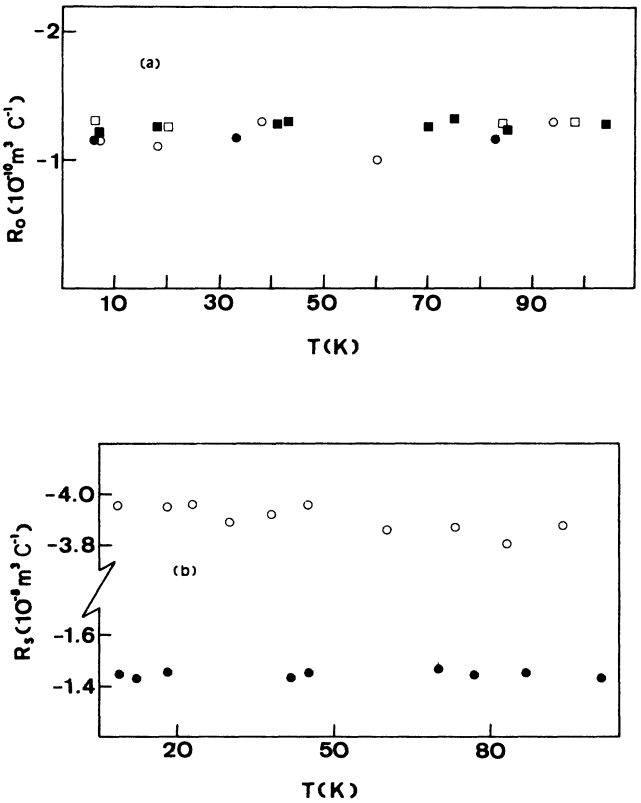

FIG. 11. (a) Ordinary Hall coefficient R_0 vs temperature for equilayered Nb/Ni films with ○, $\lambda=40$ Å; ●, $\lambda=100$ Å; ■, $\lambda=200$ Å; □, $\lambda=300$ Å. (b) Extraordinary Hall coefficient R_s vs temperature for equilayered Nb/Ni films with ○, $\lambda=40$ Å and ●, $\lambda=200$ Å.

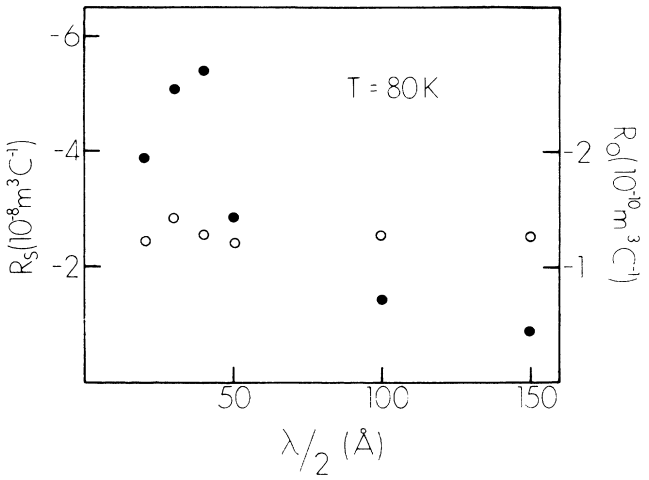

FIG. 12. Extraordinary and ordinary Hall coefficients: ●, R_s and ○, R_0 vs layer thickness for equilayered Nb/Ni films.

is the same. The clear difference in $H_K(T)$ between small and high magnetic layer thickness seems to be due, in Nb/Ni multilayers, to some dimensional effect in the Ni layers; the Nb layers only seem to play a minor effect.

Figure 11 shows the temperature dependence of the ordinary R_0 and extraordinary R_s Hall coefficients in the low temperature range. In both cases there is no temperature dependence, at least below 100 K. It is worthwhile to point out that for equilayered samples, the R_0 values are dominated by Ni and it is almost independent of the bilayer thickness. In a very crude Hall-effect model, this means that the carrier concentration could be constant for samples with a fixed Nb/Ni layer-thickness ratio. However, the R_s coefficient is wavelength dependent and its values are higher than in pure Ni (see Fig. 12). There is an enhancement of R_s for layer thickness of 40 Å. This behavior is not clear at present. Theories of Hall effect in ferromagnetic materials, with itinerant magnetic carriers,[26] predict a dependence of R_s with resistivity

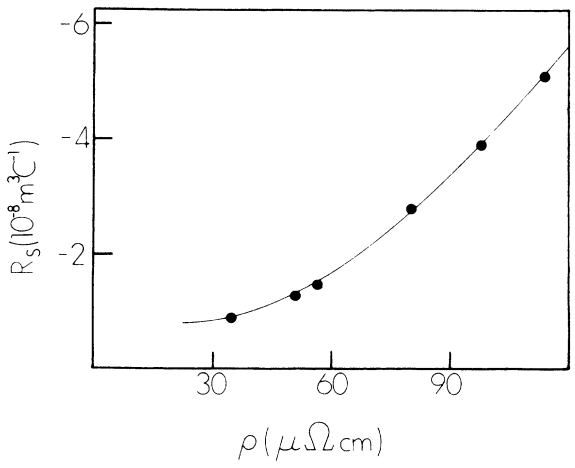

FIG. 13. Extraordinary Hall coefficient R_s vs resistivity for equilayered Nb/Ni films at $T = 100$ K.

$$R_s = a\rho + A\rho^2 .$$

Figure 13 shows that behavior for nominal equilayered films. Again the ferromagnetic character of the samples is evident.

IV. CONCLUSIONS

Nb/Ni multilayered films have been grown by dc triode sputtering. This system seems to be a promising candidate to get high-quality multilayers. X-ray data show that Nb/Ni multilayers grow with strong modulation structure. The small-angle x-ray scans show several orders of diffraction peaks, pendellösung fringes, and sharp rocking curves. The high-angle scans show a behavior similar to other largely mismatched multilayers,[13] with textured (111) fcc Ni layers and (110) bcc Nb layers for bilayer thicknesses between 40 and 1000 Å.

Resistivity measurements show localization effects analogous to those already reported in Mo/Ni multilayers.[19] The actual origin of these resistivity minima is unclear at present. The short MFP in Nb layers could play an important role in localization phenomena. For Ni layers, the possible interplay between magnetic order and localization has to be taken into account. Kondo-type mechanisms do not seem to be a clear candidate to explain localization in Nb/Ni multilayers.

Hall-effect measurements clearly show the ferromagnetic character of the samples. Independent SQUID magnetization measurements show hysteresis loops and saturation magnetizations down to 10 Å nominal Ni layer thickness. The saturation magnetic field H_s, extracted from the Hall-effect data, has a peculiar behavior following a linear dependence with temperature for very short Ni layer thicknesses. The samples have an in-plane anisotropy with an enhancement of the anisotropy field H_K values for decreasing Ni layer thicknesses. The H_K seems to be Nb layer thickness independent. The anisotropy field H_K versus temperature shows similar behavior to that of $H_s(T)$. The origin of this anisotropy and the clear dimensional effects that appear in the temperature dependence are not understood.

The anomalous Hall coefficient R_s presents an enhancement in comparison to the R_s value of pure Ni film. The resistivity values in Nb/Ni multilayers, higher than in Ni film, could explain this fact. R_s versus resistivity follows the theoretical model for itinerant ferromagnets. R_0 and R_s are temperature independent in the range 4.2–100 K, while R_s has a maximum for bilayer thickness of 80 Å, and R_0 seems to be bilayer-thickness independent.

ACKNOWLEDGMENTS

We want to thank G. Fillion (Centre National de la Recherche Scientifique, Grenoble) for the SQUID measurements and J. L. Sacedón for the Auger measurements. We also thank F. Briones, J. L. Sacedón, and J. Mendiola (Consejo Superior de Investigaciones

Cientificas) for allowing us to use their facilities. We would like to thank I. K. Schuller, C. M. Falco, D. B. McWhan, and J. P. Locquet for very useful conversations. This work was supported by Comision Asesora de Investigacion Cientifica y Tecnica and by Centro de Investigaciones Energeticas Medioambientales y Tecnologicas.

[1]*Synthetic Modulated Structures,* edited by L. L. Chang and B. C. Giessen (Academic, Orlando, 1985).
[2]I. K. Schuller, Phys. Rev. Lett. **44**, 1597 (1980).
[3]C. S. L. Chun, G. G. Zheng, J. L. Vicent, and I. K. Schuller, Phys. Rev. B **29**, 4915 (1984).
[4]M. Grimsditch, M. Khan, A. Kueny, and I. K. Schuller, Phys. Rev. Lett. **51**, 498 (1983).
[5]I. K. Schuller, in *Physics Fabrication and Applications of Multilayered Structures,* edited by P. Dhez and C. Weisbuch (Springer-Verlag, Berlin, in press).
[6]E. Bauer and J. H. van der Merwe, Phys. Rev. B **33**, 3657 (1986).
[7]D. B. McWhan, in Ref. 1, p. 48.
[8]B. M. Clemens, Phys. Rev. B **33**, 7615 (1986).
[9]M. R. Khan, C. S. L. Chun, G. P. Felcher, M. Grimsditch, A. Kueny, C. M. Falco, and I. K. Schuller, Phys. Rev. B **27**, 7186 (1983).
[10]C. F. Majkrazk, Physica B + C **136B**, 69 (1986).
[11]L. Tapfer and K. Ploog, Phys. Rev. B **33**, 5565 (1986).
[12]J. M. Murduck, J. L. Vicent, I. K. Schuller, and J. B. Ketterson, J. Appl. Phys. **62**, 4216 (1987); H. Homma, S. Lepetre, J. M. Murduck, and I. K. Schuller, Soc. Photo-Opt. Instrum. Eng. Proc. **563**, 150 (1983).
[13]B. M. Clemens and J. G. Gay, Phys. Rev. B **35**, 9337 (1987).
[14]W. P. Lowe, T. W. Barbee, Jr., T. H. Geballe, and D. B. McWhan, Phys. Rev. B **24**, 6193 (1981).
[15]P. F. Carcía, A. Suna, D. G. Onn, and R. van Antwerp, Superlatt. Microstruct. **1**, 101 (1985).
[16]P. R. Broussard and T. H. Geballe, Phys. Rev. B **35**, 1664 (1987).
[17]K. Meyer, I. K. Schuller, and C. M. Falco, J. Appl. Phys. **52**, 5803 (1981); R. P. Somekh, J. Vac. Sci. Technol. A **2**, 1285 (1984).
[18]C. M. Falco and I. K. Schuller, in Ref. 1, p. 343.
[19]C. Uher, R. Clarke, G. G. Zheng, and I. K. Schuller, Phys. Rev. B **30**, 453 (1984).
[20]G. S. Grest and S. R. Nagel, Phys. Rev. B **19**, 3571 (1979).
[21]M. Gurvitch, Phys. Rev. B **34**, 540 (1986).
[22]L. R. Testardi and L. F. Mattheiss, Phys. Rev. Lett. **41**, 1612 (1978).
[23]T. R. Werner, I. Banarjee, Q. S. Yang, C. M. Falco, and I. K. Schuller, Phys. Rev. B **26**, 2224 (1982).
[24]P. W. Anderson, E. Abrahams, and T. V. Ramakrishnan, Phys. Rev. Lett. **43**, 718 (1979).
[25]B. L. Altshuler, A. G. Aranov, and P. A. Lee, Phys. Rev. Lett. **44**, 1288 (1980).
[26]C. M. Hurd, *The Hall Effect in Metals and Alloys* (Plenum, New York, 1972).
[27]G. Bergmann, Phys. Rev. Lett. **41**, 264 (1978).
[28]I. K. Schuller and M. Gimsditch, J. Appl. Phys. **55**, 2491 (1984).
[29]E. M. Gyorgy, J. F. Dillon, Jr., D. B. McWhan, L. W. Kupp, Jr., L. K. Testardi, and P. J. Flanders, Phys. Rev. Lett. **45**, 57 (1980).